

TPSR of CO hydrogenation on Co/Nb₂O₅/Al₂O₃ catalysts

F.M.T. Mendes^{a,1}, C.A.C. Perez^a, F.B. Noronha^b, M. Schmal^{a,*}

^aFederal University of Rio de Janeiro, NUCAT-PEQ-COPPE, Bl. G-128, Centro de Tecnologia, Cidade Universitária, Rio de Janeiro, Brazil

^bInstituto Nacional de Tecnologia, Av. Venezuela, 2, CEP 20081-310, Brazil

Available online 18 January 2005

Abstract

This study involves the characterization of a series Co/*x*% Nb₂O₅/Al₂O₃ catalysts.

The temperature-programmed surface reaction technique (TPSR) and in situ diffuse reflectance spectroscopy (DRS) results have shown a transient behavior of the catalysts, distinguishing very well the Co/Al₂O₃ from the Co/Nb₂O₅/Al₂O₃ catalysts.

DRS and temperature-programmed reduction (TPR) results indicate the presence of Co²⁺, besides Co⁰ and Co⁰–NbO_{*x*}, which affect greatly the performance of the catalysts.

These results allowed us to propose that the interface Co²⁺–Co⁰ is responsible for the methanation reaction, while the Co⁰–NbO_{*x*} is responsible for the hydrocarbon chain grow. The relative amount of each specie on the surface plays a fundamental role on the selectivity behavior of CO hydrogenation.

© 2004 Elsevier B.V. All rights reserved.

Keywords: CO hydrogenation; Niobia; Cobalt; Niobia/alumina

1. Introduction

The reduction reserves and high crude oil prices make alternative routes for the production of petroleum derivatives and raw materials attractive. CO hydrogenation product spectrum includes hydrocarbons from methane to wax, depending on catalyst selection. In this context, cobalt-based catalysts have been applied worldwide for Fischer–Tropsch synthesis (FT) [1]. The polymerization nature of the FT conversion imposes constraints on selectivity manipulation, such as the product distribution by the conventional FT catalyst (selectivities for gasoline or diesel fuel) are relatively low [2]. Reducible support such as niobia [3–8] and titania [9,10] have been used in order to overcome the selectivity limitations. A high selectivity toward long chain hydrocarbons in the FT synthesis after reduction at high temperature was observed over Co/Nb₂O₅ [3–8] and Ni/Nb₂O₅ [9] catalysts. These results might be explained by the formation of new sites involving the metal and the partially reduced support during high temperature reduction.

The anchoring of niobia over large surface area supports favors the enhancement of metal dispersion, since niobia itself exhibits low surface area. One important question arises, whether the niobium oxide when dispersed over a support with high surface area affects the surface properties and consequently the activity or the product distribution of the CO hydrogenation. Ko et al. [9] compared the Nb₂O₅ and Nb₂O₅–SiO₂-supported nickel catalyst on CO hydrogenation. They expected to obtain the same SMSI extent on both systems, since there was sufficient supply of niobia. However, the catalytic activity of a Ni–Nb₂O₅ was 50% greater than on a Ni–Nb₂O₅–SiO₂ system. They could not totally rule out the possibility of some crystallites sitting on uncovered SiO₂ contributing to the chemistry. They found that such an effect was small and suggested the lower availability of Nb₂O₅ in the Nb₂O₅–SiO₂ system.

Different niobium oxide precursors and preparation methods have been used for the preparation of supported niobium oxide catalysts such as: (i) aqueous impregnation with niobium oxalate [11,12]; impregnation of niobium ethoxide using organic solvents [13,14]; chemical vapor deposition of niobium ethoxide or niobium pentachloride [15]. The niobium oxalate possesses low solubility in aqueous solutions, which can be increased by the addition of

* Corresponding author. Fax: +55 21 2906626.

E-mail address: schmal@peq.coppe.ufrj.br (M. Schmal).

¹ Present address: Fritz-Haber Institut, Berlin, Germany.

oxalic acid. However, the niobium oxalate and the oxalic acid precipitate from solution at high oxalic acid concentrations. The use of niobium ethoxide or niobium pentachloride requires a controlled environment and special procedures to avoid the decomposition of the precursor in the presence of water and to control the density of surface hydroxyls groups. The preparation of supported niobium oxide catalysts using an ammonium complex of niobium as a precursor is not so usual [16]. This precursor salt is easily solubilized in water at room temperature.

The preparation method and niobium precursors do not affect the molecular structures of surface niobia species, but they determine their dispersion [17]. The nature of the precursor had a strong effect on the distribution of the niobium oxide species over the alumina and consequently, on the reduction of niobium oxide species [18]. We prepared $\text{Nb}_2\text{O}_5/\text{Al}_2\text{O}_3$ materials by using two different precursors salts: niobium ammonium complex and niobium oxalate salt [18]. The results showed that the niobium precursor influence the species growing leading to phases with different reducibility. The XPS revealed the presence of multilayers of niobium oxide on the $\text{Nb}_2\text{O}_5/\text{Al}_2\text{O}_3$ samples prepared by using niobium ammonium complex while the ones obtained from niobium oxalate led to Nb_2O_5 particles islands. Therefore, the nature of the precursor affected significantly the reduction of niobium oxide species. The $\text{Nb}_2\text{O}_5/\text{Al}_2\text{O}_3$ (niobium oxalate salt) samples exhibited a high reducibility due to the lower interaction between the niobium oxide species of the islands and the support.

Afterwards, we studied the performance of Co supported on $\text{Nb}_2\text{O}_5/\text{Al}_2\text{O}_3$ prepared by ammonium complex on FT synthesis. The activity of the $\text{Co}/\text{Nb}_2\text{O}_5/\text{Al}_2\text{O}_3$ catalyst was compared to $\text{Co}/\text{Al}_2\text{O}_3$ and $\text{Co}/\text{Nb}_2\text{O}_5$ catalysts [8]. The catalytic results showed that after reduction at 773 K, the $\text{Co}/\text{Nb}_2\text{O}_5$ catalyst presented a low methanation activity and a high selectivity for long chain hydrocarbons in the CO hydrogenation. On the other hand, the performance of $\text{Co}/\text{Al}_2\text{O}_3$ and $\text{Co}/5\% \text{Nb}_2\text{O}_5/\text{Al}_2\text{O}_3$ was quite similar, after reduction at 573 or 773 K. However, the increase of Nb_2O_5 content ($\text{Co}/20\% \text{Nb}_2\text{O}_5/\text{Al}_2\text{O}_3$) changed the selectivity of the reaction, presenting the same product distribution observed for the $\text{Co}/\text{Nb}_2\text{O}_5$ catalyst, but the effect was less pronounced on the niobia-promoted $\text{Co}/\text{Al}_2\text{O}_3$ than on the $\text{Co}/\text{Nb}_2\text{O}_5$ catalyst.

The goal of this was to study $\text{Co}/x\% \text{Nb}_2\text{O}_5/\text{Al}_2\text{O}_3$ catalysts by temperature-programmed reduction (TPR), diffuse reflectance spectroscopy (DRS) techniques and CO hydrogenation by temperature-programmed reaction (TPSR) as a potential catalyst to CO hydrogenation.

2. Experimental

2.1. Catalyst preparation

The niobium ammonium complex obtained from CBMM (Companhia Brasileira de Metalurgia e Mineração (CBMM,

Table 1

Surface areas (BET) and contents of Nb_2O_5 and cobalt

Sample	BET area (m^2/g)	Nb_2O_5 content (%)	Co content (%)
$\text{Co}/\text{Al}_2\text{O}_3$	187	4.25	4.25
$\text{Co}/\text{Nb}_2\text{O}_5$	13	4.50	4.50
$\text{Co}/5\% \text{Nb}_2\text{O}_5/\text{Al}_2\text{O}_3$	201	4.3	
$\text{Co}/10\% \text{Nb}_2\text{O}_5/\text{Al}_2\text{O}_3$	196	9.45	
$\text{Co}/20\% \text{Nb}_2\text{O}_5/\text{Al}_2\text{O}_3$	178	19.9	4.80
$\text{Co}/30\% \text{Nb}_2\text{O}_5/\text{Al}_2\text{O}_3$	150	31.3	

AD 1264)) was calcined at 873 K at a heating rate of 2 K/min for 4 h, which produced the crystalline TT or T form of niobium pentoxide. Alumina was pretreated in aerated furnace (50 ml/min) at 823 K for 16 h.

The $x\% \text{Nb}_2\text{O}_5/\text{Al}_2\text{O}_3$ ($x = 5, 10, 20$ and $30 \text{ wt.}\%$ of Nb_2O_5) was prepared by wet impregnation of alumina with a solution of an niobium ammonium complex in a rotator evaporator for 16 h. After drying at 353 K, under vacuum, the sample was dried at 373 K for 16 h, followed by calcination under flowing air at 823 K (2 K/min) for 16 h.

The cobalt catalyst was prepared by incipient wetness impregnation with a $\text{Co}(\text{NO}_3)_2 \cdot 6\text{H}_2\text{O}$ (Riedel-de H  en, 99% purity) solution. The Co content was approximately 5 wt.%. After impregnation, all catalysts were dried overnight at 383 K followed by calcination at 2 K/min up to 673 K and kept for 3 h. Table 1 shows cobalt concentrations determined by atomic absorption and the corresponding BET surface areas of the catalysts.

2.2. Catalyst characterization

2.2.1. Diffuse reflectance spectroscopy (DRS)

Diffuse reflectance spectra were recorded in the range of 200–900 nm using an UV–Vis–NIR spectrophotometer (Cary 5E, Varian) equipped with an integrating sphere (Harrick). The alumina, niobia and $\text{Nb}_2\text{O}_5/\text{Al}_2\text{O}_3$ samples were used as reference for the $\text{Co}/\text{Al}_2\text{O}_3$, $\text{Co}/\text{Nb}_2\text{O}_5$ and $\text{Co}/\text{Nb}_2\text{O}_5/\text{Al}_2\text{O}_3$ samples, respectively.

The DRS spectra were recorded on both calcined and pretreated samples. Samples were pretreated in the chamber passing He flow at 5 K/min up to 423 K for 30 min and cooled to room temperature for analysis. Then, the flow was switched to a reduction mixture of 10% H_2/Ar (20 ml/min) and the sample was heated up to 573 or 773 K and kept, at this temperature, for 30 min. After that, the sample was cooled to RT for spectral acquisitions.

2.2.2. Temperature-programmed reduction (TPR)

Temperature-programmed reduction (TPR) was conducted using a conventional apparatus equipped with a thermal conductivity detector. Each sample was pre-treated in an argon flow at 383 K, for 30 min, and cooled down to room temperature. The reduction was performed by heating the sample from 298 up to 1373 K at a rate of 8 K/min using a 1.75% H_2/Ar mixture flow.

2.2.3. Temperature-programmed surface reaction (TPSR)

The temperature-programmed surface reaction analysis was performed in glass micro reactor at atmospheric pressure. The catalyst (0.5 g) was previously reduced with pure hydrogen at 573 or 773 K during 16 h and then cooled to room temperature. Then, a reaction mixture containing $H_2/CO = 2$ was passed through the catalyst at 30 ml/min and the temperature was raised at a heating rate of 20 K/min up to 773 K. Samples were collected in a multiloop valve (VCI-Valco) at different temperatures and were analyzed on line in a TCD chromatograph (Varian-STAR 3400) using a Porapak Q column.

3. Results and discussions

3.1. Diffuse reflectance UV–Vis (DRS)

Figs. 1 and 2 display the DRS spectra of the calcined and reduced catalysts, respectively. The calcined Co/Al_2O_3 spectrum presented two strong absorption bands at 402 and 700 nm and a shoulder at 458 nm. According to the literature, the absorption bands at 435 and 642 nm for the $Co/\alpha-Al_2O_3$ system were ascribed to $^1A_{1g} \rightarrow ^1T_{2g}$ and $^1A_{1g} \rightarrow ^1T_{1g}$ transitions of octahedral coordinated Co^{3+} ions [19]. Furthermore, Chung and Massoth [20] assigned to an octahedrally coordinated Co^{2+} the broad band around 500 nm on Co/Al_2O_3 catalysts. Ashley and Mitchell [21] performed DRS analyses on model compounds containing cobalt in octahedral and tetrahedral coordination. They observed marked differences between octahedral (CoO) and tetrahedral ($CoAl_2O_4$) Co^{2+} species. In particular, the Co^{2+} in octahedral coordination displays a band at higher frequency (534 nm) than the Co^{2+} in tetrahedral coordination (558, 595 and 634 nm). Thus, in our work, the bands at 402 and 700 nm can be attributed to Co^{3+} in octahedral coordination, whereas the shoulder observed around 458 nm corresponds to octahedral Co^{2+} species.

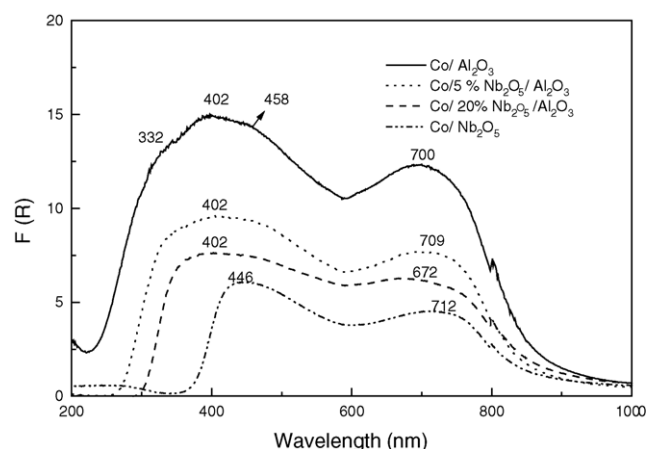


Fig. 1. DRS spectra of calcined catalysts.

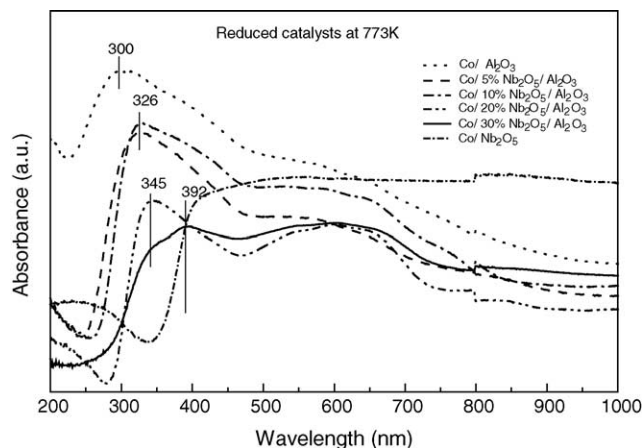


Fig. 2. DRS spectra of reduced catalysts at 773 K.

DRS spectra of the catalysts containing 5 and 20 wt.% Nb_2O_5 catalysts show broad bands at 402/709 and 402/672 nm, respectively. The spectral features were similar to those of the Co/Al_2O_3 catalyst. The triplet bands assigned to tetrahedral Co^{2+} species were not observed in the spectrum.

DRS spectra of 5% Co/Nb_2O_5 exhibited bands at 446 and 712 nm. Noronha et al. [22] found that the bands around 446 and 712 nm could be attributed to octahedral Co^{3+} and Co^{2+} species. It is important to stress that the shoulder around 300 nm and the band at 400 nm were not observed here, which suggests that the shoulder and band may be only assigned to surface cobalt species in a intimate contact with the alumina support.

Fig. 2 shows the DRS spectra after reduction at 773 K. The cobalt species were partially reduced, and the band seen at 300 nm is assigned to tetrahedral Co^{2+} species. The triplet band around 546, 598 and 668 nm were also observed, being more clear to the $Co/30\% Nb_2O_5/Al_2O_3$ catalyst (Fig. 2). The band near 300 nm still remains after the reduction treatment. The addition of niobia shifted the band at 300 nm towards higher wavelength, compared to the Co/Al_2O_3 catalyst, while its intensity (band 300 nm) decreased with increasing amount of niobia. These results suggest that the amount of cobalt species, which are in contact with the alumina support, affect the intensity bands and therefore the coordination of Co species.

3.2. Temperature-programmed reduction (TPR)

TPR profiles of different catalysts are shown in Fig. 3. Co/Al_2O_3 displays three reduction peaks at 593, 704 and 943 K. The TPR profiles with increasing Nb_2O_5 content changed with higher content. The 20% Nb_2O_5 displays one peak at reduction temperature of 680 K and another smaller peak around 913 K. With 30% Nb_2O_5 it shows one reduction peak at low temperature 511 K, besides two others at 690 and 943 K. Again the Co/Nb_2O_5 catalyst shows also three reduction peaks at 647, 696 and 815 K.

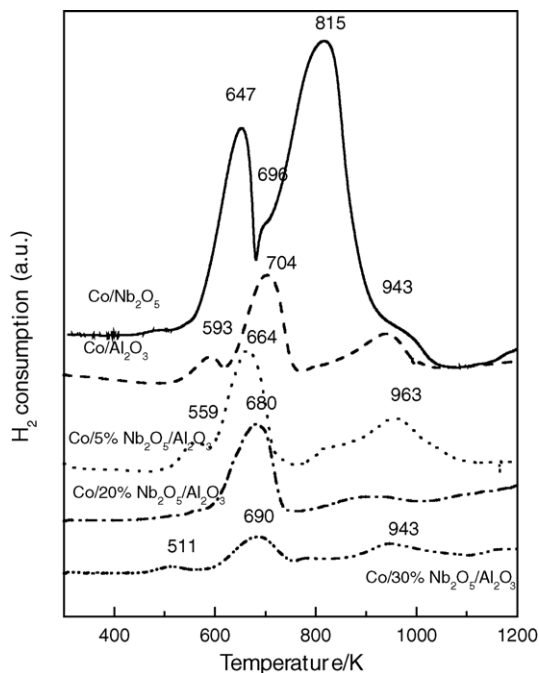


Fig. 3. TPR profiles of Co/Al₂O₃, Co/Nb₂O₅/Al₂O₃ and Co/Nb₂O₅.

There are three different cobalt species identified in the Co/Al₂O₃:Co₃O₄ particles, Co²⁺ species and a spinel structure of CoAl₂O₄ [23,24]. The peaks at lower temperature can be attributed to the reduction of Co₃O₄ in two stages, while the reduction at 943 K is related to the reduction of surface Co²⁺ species with strong interaction with the alumina support.

Niobium is a reducible oxide and its partial reduction can be proved by performing TPR measurements, which has already been published before [18,22]. Noronha et al. [22] applied DRX, DRS, XPS and TPR techniques in order to investigate the different types of cobalt species over the niobium support. Based on TPR, DRS and XPS they identified mainly the presence of Co²⁺ and Co₃O₄ surface species. They have shown that the relative amount of each specie varies according to the cobalt metal loading. For example, at a high cobalt content (>8 wt.%), Co₃O₄ are the main species whereas the percentage of Co²⁺ species linked to the support increases as the cobalt loading decreases. Furthermore, based on XPS data, these Co²⁺ species were represented by the partial reduction of Co₃O₄ to Co²⁺ and by a mixture of niobate phases (Co₂Nb₅O₁₄ and CoNb₂O₆).

Based on the literature [22], in our case, the lower reduction peak at 647 K of Co/Nb₂O₅ sample could also be attributed to the reduction of Co³⁺ → Co²⁺ and the shoulder around 696 K and above at 815 K to the reduction of Co²⁺ species and the support.

The Co/20% Nb₂O₅/Al₂O₃ sample shows only one peak at 680 K, corresponding to the reduction of Co²⁺ species. In this case it seems that Co²⁺ are the prevailing surface species, because the reduction peak at low temperature was not observed.

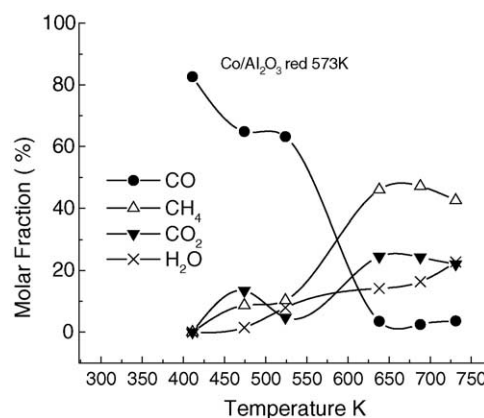


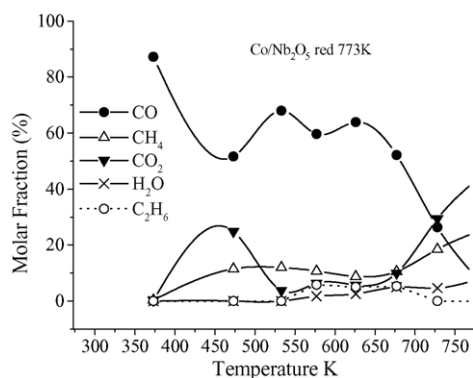
Fig. 4. TPSR on Co/Al₂O₃ reduced at 773 K.

The Co/30% Nb₂O₅/Al₂O₃ shows again the reduction of Co₃O₄ particles and Co²⁺ species besides the reduction of Nb₂O₅ at the surface.

4. TPSR analysis

Fig. 4 displays the TPSR profiles of the Co/Al₂O₃ catalyst after reduction at 573 K, when the temperature rises from RT up to 773 K. Similar results were obtained for this catalyst reduced at 773 K. The reaction starts at around 400 K. CO is consumed with the simultaneous formation of CO₂ and CH₄ up to 474 K. However, between 474 and 534 K, CO consumption does not change and the molar fraction of CO₂ decreases, while the fraction of water and methane increases. The decrease of CO consumption is probably due to the deactivation and coke formation. Above 525 K, the molar fraction of CO decreases abruptly until almost complete consumption, while methane and CO₂ and water formation increase also significantly. Methane is the principal product of reaction above 500 K, and together with CO₂ reaches a maximum value around 641 K, with increasing water formation. In conclusion, there are two domains of reaction below and above 525 K. In this case, the drastic increase of CH₄, CO₂ and water is noteworthy.

On the other hand, when the Co/Nb₂O₅ catalyst was reduced at 773 K it exhibited three domains of reaction, as presented in Fig. 5. One region at low temperatures, where a considerable consumption of CO was observed, up to 460 K. The main products were CO₂, methane and water. The second region, between 525 and 670 K shows that the CO concentration is constant and a third region, where the reaction takes place and the CO consumption increases again. This behavior would suggest important transient modification at the surface, with an SMSI effect, and then reactivation of the catalyst. Indeed, Nb₂O₅ is a reducible oxide, which at 773 K favors the formation of NbO_x species migrating over Co sites. Hoffer et al. [25] have also observed this SMSI effect for a Pt/Nb₂O₅/Al₂O₃ catalyst. The destruction of these patches is attributed to the presence

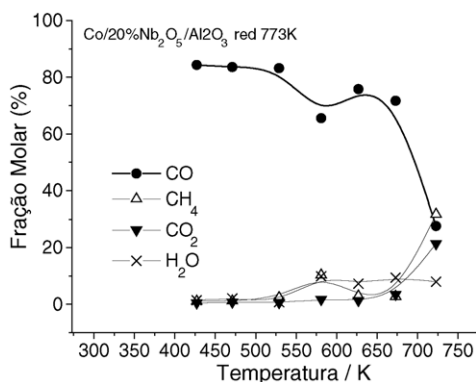
Fig. 5. TPSR on Co/Nb₂O₅ reduced at 773 K.

of water during the reaction, recovering partially the active surface sites. Between this temperatures range CH₄ concentration is extremely low with a little ethane formation. However, above 670 K the reaction proceeds very fast with the formation of CO₂ being the main product around 40%. This explains the recovery of surface active sites, which can be attributed to the destruction of the SMSI effect in the presence of water during the reaction.

Fig. 6 displays the TPSR profile of the Co/20% Nb₂O₅/Al₂O₃ reduced at 773 K. Unlike the other catalysts, this one did not display CO consumption until 525 K, and the reaction increases slowly up to 585 K with little formation of CH₄ and H₂O. Similar to the Co/Nb₂O₅, it exhibits a similar transient behavior between 525 and 670 K, indicating a dynamic sequential process of deactivation and activation and only above 640 K the reaction is faster. The behavior of Co/5% Nb₂O₅/Al₂O₃ and Co/10% Nb₂O₅/Al₂O₃ catalysts are quite similar to the Co/Al₂O₃.

The TPSR profile shows two peaks for methane formation, which is in accordance with results reported by Lee and Bartholomew [26], although they used different methodology, namely adsorbing H₂ first and then flowing CO or flowing both simultaneously and then raising the temperature.

Lee and Bartholomew [26] suggested a reaction mechanism, which they attributed the first peak to the

Fig. 6. TPSR on Co/20% Nb₂O₅/Al₂O₃ reduced at 773 K.

formation of methane on big Co⁰ crystallites, while the second one to methane, however, through CH_xO species formation on the support due to spillover followed by decomposition of these species on metallic particles due to back spillover.

The TPSR results on the Co/Nb₂O₅ showed that after an initial reaction at lower temperatures the catalyst suffers deactivation and then an activation process, which can be explained by the SMSI effect and not by the coke formation. Indeed, Nb₂O_x species present at the interface migrate over Co⁰ with the formation of patches, blocking metallic surface sites. However, with the formation of water during the reaction, as reported by Kunimori et al. [27] and Haller and Resasco [28] it cleans up the surface, removing partially the Nb₂O_x species from metallic Co⁰ surface, and probably built new interfacial sites with the formation of Co⁰-Nb₂O_x site. The behavior of the catalysts containing 20, 30 wt.% Nb₂O₅ or more, exhibit similar behavior as the Co/Nb₂O₅ catalyst, but are less active. DRS results of these catalysts showed bands shift toward higher wavelength compared to the Co/Al₂O₃ catalyst. A triplet was observed for higher concentrations of niobia, which suggests still but less cobalt species at the alumina support, compared to the Co/Nb₂O₅ catalyst itself.

Frydman et al. [29] performed CO hydrogenation over 2% Co/Nb₂O₅ catalyst. Basically, it was observed only the methane formation and hydrocarbons in the C₂–C₄ range. This low metal loading catalyst have been characterized by the predominance of Co²⁺ on the surface. Recently, Guzzi et al. [30] have reported high methane selectivity in CO hydrogenation over Co and Re–Co catalysts prepared by sol/gel technique. Those samples were partially reduced (32% degree of reduction) and presented also a predominance of Co²⁺ species.

In summary, based on DRS, TPR, TPSR and the selectivity behavior towards CO hydrogenation [8] we could verify that Co/Al₂O₃ catalyst has a predominance of exposed Co²⁺ besides Co⁰ sites and behave mainly as a methanation catalyst. On the other hand, Co/Nb₂O₅, after reduction at 773 K, presents low methanation activity and the hydrocarbon chain grown is observed. Furthermore, the activity and selectivity of different Co/Nb₂O₅/Al₂O₃ catalyst is not significantly change for low niobia contents. For lower contents they approach the Co/Al₂O₃ catalyst and for higher contents (20%) the Co/Nb₂O₅ catalyst. Then, the following sites should be present on the surface of our catalysts:

- For Co/Al₂O₃ (case 1): Two reaction sites—site A for Co⁰ after the reduction of big Co₃O₄ crystallites and sites B for interfacial (Co⁰/Co²⁺) sites. CO dissociates on sites A with the formation of α-carbon, which is than hydrogenated to CH₄, in agreement with the proposed model of Lee and Bartholomew [26]. However, sites B form methoxy species on Co²⁺ species with further backspillover to Co⁰, followed by decomposition to methane.

These sites are mainly responsible for the methanation reaction.

- For Co/Nb₂O₅ (case 2): Three reaction sites—sites A and B similar as case 1, and sites C at the interface of Co⁰/NbO_x. Sites C for Co/Nb₂O₅ catalyst favor the growth of hydrocarbon chains.
- For Co/Nb₂O₅/Al₂O₃ (case 3): Similar to cases 1 and 2, depending on the niobia content.

5. Conclusions

The TPSR technique supported by DRS results has shown a transient behavior of the catalysts, indicating a dynamic sequential process of deactivation and activation, distinguishing very well the Co/Al₂O₃ from the Co/Nb₂O₅ catalysts. In addition, there are no significant changes with the coated Co/Nb₂O₅/Al₂O₃.

DRS results and TPR results indicate the presence of Co²⁺ at the surface, in addition to Co⁰ and interfacial Co⁰–NbO_x, which greatly affect the performance of the catalyst with respect to selectivity towards methane and higher carbon chains. The behavior is different on Al₂O₃ and Nb₂O₅ supports, depending on the temperature of reduction.

The Co²⁺ species still remain in contact with Al₂O₃ even with the addition of higher niobium contents.

The interface Co⁰/Co²⁺ is mainly responsible for the methanation reaction, while the interface Co⁰–NbO_x is responsible for the hydrocarbon chain grown.

References

- [1] R.B. Anderson, *The Fischer–Tropsch Synthesis*, Academic Press, Orlando, 1984.
- [2] D. Schenke, *New Trends of Methane Activation*, Elsevier, 1990.
- [3] R.R.C.M. Silva, J.A. Dalmon, R. Frety, M. Schmal, *J. Chem. Soc., Faraday Trans. 89* (1993) 3975.
- [4] A. Frydman, R.R. Soares, M. Schmal, *Stud. Surf. Sci. Catal.* 75 (1993) 2796.
- [5] R.R. Soares, A. Frydman, M. Schmal, *Catal. Today* 16 (1993) 361.
- [6] F.B. Noronha, A. Frydman, D.A.G. Aranda, C.A. Perez, R.R. Soares, B. Moraweck, D. Castner, C.T. Campbell, R. Frety, M. Schmal, *Catal. Today* 28 (1996) 147.
- [7] F. Mendes, F.B. Noronha, R.R. Soares, C.A.C. Perez, G. Marchetti, M. Schmal, *Stud. Surf. Sci. Catal.* 136 (2001) 177.
- [8] F.T. Mendes, F.B. Noronha, M. Schmal, *Stud. Surf. Sci. Catal.* 130 (2001) 3717.
- [9] E.I. Ko, M. Hupp, K. Foger, *J. Catal.* 86 (1984) 315.
- [10] E. Iglesia, S.L. Soled, A. Fiato, G.H. Via, *J. Catal.* 143 (1993) 345.
- [11] E. Iglesia, *Appl. Catal. A: Gen.* 161 (1997) 59.
- [12] J.M. Jehng, I.E. Wachs, in: *Proceedings of the Symposium on New Catalytic Materials and Techniques*, Miami Beach, 1989, p. 546.
- [13] K. Asakura, Y. Iwasawa, *J. Phys. Chem.* 95 (1991) 1711.
- [14] N. Ichikuni, Y. Iwasawa, *J. Phys. Chem.* 98 (1994) 11576.
- [15] C.L.T. da Silva, V.L.L. Camorim, J.L. Zotin, M.L.R.D. Pereira, A.C. Faro Jr., *Catal. Today* 57 (2000) 209.
- [16] M.M. Pereira, E.B. Pereira, Y.L. Lam, M. Schmal, *Catal. Today* 57 (2000) 291.
- [17] I.E. Wachs, L.E. Briand, J.M. Jehng, L. Burcham, X. Gao, *Catal. Today* 57 (2000) 323.
- [18] F.T. Mendes, C.A. Perez, R.R. Soares, F.B. Noronha, M. Schmal, *Catal. Today* 78 (2003) 449.
- [19] A.S. Sass, V.A. Shvets, G.A. Svel'eva, U.B. Kasanskii, *Kinet. Catal.* 26 (5) (1985) 1149.
- [20] K.S. Chung, F.E. Massoth, *J. Catal.* 64 (1980) 320.
- [21] J.H. Ashley, P.C.H. Mitchell, *J. Chem. Soc. A* 2821 (1968).
- [22] F.B. Noronha, C.A. Perez, M. Schmal, R. Fréty, *Phys. Chem. Chem. Phys.* 1 (1999) 2861.
- [23] P. Arnoldy, A. Moulijn, *J. Catal.* 93 (1985) 38.
- [24] H. Tung, C. Yeh, C. Hong, *J. Catal.* 122 (1990) 211.
- [25] T. Hoffer, S. Dobos, L. Gucci, *Catal. Today* 16 (1993) 435.
- [26] W.H. Lee, C.H. Bartholomew, *J. Catal.* 120 (1989) 256.
- [27] K. Kunimori, H. Abe, E. Yamaguchi, S. Matsui, T. Uchijima, in: *Proceedings of the Eighth International Congress on Catalysis*, 1984, p. 251.
- [28] G. Haller, D.E. Resasco, *Adv. Catal.* 36 (1989) 173.
- [29] A. Frydman, D.G. Castner, C.T. Campbell, M. Schmal, *J. Catal.* 188 (2) (1999) 1.
- [30] L. Gucci, G. Stefler, L. Borkó, Zs. Koppány, F. Mizukami, M. Toba, S. Niwa, *Appl. Catal. A: Gen.* 246 (2003) 79.